# INTERPLAY BETWEEN CORTICAL ADHESION AND MEMBRANE BENDING REGULATES THE FORMATION OF MICROPARTICLES

ELECTRONIC SUPPLEMENTARY INFORMATION

**Arijit Mahapatra**[a,c], **Sage A. Malingen**[a,d], **and Padmini Rangamani** [a,b*]
[a]Department of Mechanical and Aerospace Engineering, University of California San Diego,
9500 Gilman Drive, La Jolla, CA 92093, U.S.A.
[b]Department of Pharmacology, University of California San Diego,
La Jolla CA 92093-0636, U.S.A.
[c]Gamma Technolgies, LLC, Westmont, IL 60559, U.S.A.
[d]Department of Biology, University of Washington
Email addresses of corresponding author: prangamani@health.ucsd.edu

## Model Development

### Surface representation

The surface is parameterized by a position vector $\boldsymbol{r}(\theta^\alpha, t)$, where $\theta^\alpha$ are the surface coordinates, $\alpha \in \{1, 2\}$. Here we considered two different parameterizations, orthogonal Monge and axisymmetric polar coordinates. In the Monge parametrization the membrane is modeled from its projected plane and $\theta^\alpha$ are $(x, y)$, position is given by

$$\boldsymbol{r}(x, y, t) = x\boldsymbol{i} + y\boldsymbol{j} + z(x, y, t)\boldsymbol{k}, \tag{S1}$$

Where unit vectors $(\boldsymbol{i}, \boldsymbol{j}, \boldsymbol{k})$ form a fixed Cartesian orthonormal basis, and $z(x, y, t)$ is the deflection from the $(x, y)$ plane. In axisymmetric coordinates, we parameterize the membrane by the arclength $s$ and the rotation angle $\theta$ (Figure 4a) as

$$\boldsymbol{r}(r, z, \theta) = \boldsymbol{r}(s, \theta). \tag{S2}$$

The surface tangents are given by $\boldsymbol{e}_\alpha = \boldsymbol{r}_{,\alpha}$ and the surface metric $a_{\alpha\beta} = \boldsymbol{e}_\alpha \cdot \boldsymbol{e}_\beta$ and the curvature tensor $b_{\alpha\beta} = \boldsymbol{e}_{\alpha,\beta} \cdot \boldsymbol{n}$ are the two fundamental tensors we use in the derivation that follows. We refer the reader to [1, 2] for details of these derivations. The scalar invariants, mean curvature $H$, and Gaussian curvature $K$ denote the average and product of the two principal curvatures and are given by

$$H = \frac{1}{2} a^{\alpha\beta} b_{\alpha\beta}, \quad K = \frac{1}{2} \varepsilon^{\alpha\beta} \varepsilon^{\mu\delta} b_{\alpha\mu} b_{\beta\delta}, \tag{S3}$$

where, $a^{\alpha\beta} = (a_{\alpha\beta})^{-1}$, and $\varepsilon^{\alpha\beta}$ is the permutation tensor: $\varepsilon^{12} = -\varepsilon^{21} = 1/\sqrt{a}, \varepsilon^{11} = \varepsilon^{22} = 0$, with $a = \det |a_{\alpha\beta}|$. Here $\alpha, \beta, \delta, \mu$ are the surface coordinates, and moving forward we use Greek letters to indicate surface coordinates.

### Force balance

The force balance equation of the membrane is dictated by

$$\boldsymbol{T}^\alpha_{;\alpha} + p\boldsymbol{n} + \boldsymbol{f} = 0\,, \tag{S4}$$

where $p$ is normal pressure on the membrane, $\boldsymbol{f}$ applied force density on the membrane, and $()^\alpha_{;\alpha}$ is the surface divergence, and $\boldsymbol{T}$ is the traction on the membrane and given by,

$$\boldsymbol{T}^\alpha = N^{\beta\alpha}\boldsymbol{a}_\beta + S^\alpha \boldsymbol{n}. \tag{S5}$$

$\boldsymbol{N}$ is the in-plane component of the stress and is given by

$$N^{\beta\alpha} = \pi^{\beta\alpha} + \zeta^{\beta\alpha} + b^\beta_\mu M^{\mu\alpha} \qquad \text{and} \qquad S^\alpha = -M^{\alpha\beta}_{;\beta}\,, \tag{S6}$$

where $\pi^{\alpha\beta} = \nu[v^{\alpha}_{;\beta} + v^{\beta}_{;\alpha} - 2wb^{\alpha\beta}]$, is the viscous stress with $v, w$ as tangential and normal velocity, $\zeta^{\beta\alpha}$ and $M^{\beta\alpha}$ are obtained from the following constitutive relations [3]

$$\zeta^{\beta\alpha} = \rho\left(\frac{\partial F}{\partial a_{\alpha\beta}} + \frac{\partial F}{\partial a_{\beta\alpha}}\right) \quad \text{and} \quad \boldsymbol{M}^{\beta\alpha} = \frac{\rho}{2}\left(\frac{\partial F}{\partial b_{\alpha\beta}} + \frac{\partial F}{\partial b_{\beta\alpha}}\right), \tag{S7}$$

with $F = W/\rho$ as the energy mass density of the membrane. Combining these we get the balance equations in equation S4 in normal direction

$$\begin{aligned} p + \boldsymbol{f}\cdot\boldsymbol{n} = -(S^{\alpha}_{;\alpha} + N^{\beta\alpha}b_{\beta\alpha}) &= \Delta\left(\frac{1}{2}W_H\right) + (W_K)_{;\alpha\beta}\,\tilde{b}^{\alpha\beta} \\ &+ W_H\left(2H^2 - K\right) + 2H\left(KW_K - W\right) - 2\lambda H \\ &- 2\nu\big[b^{\beta\alpha}d_{\beta\alpha} - w(4H^2 - 2K)\big], \end{aligned} \tag{S8}$$

with $\tilde{b}^{\alpha\beta} = 2aa^{\alpha\beta} - b^{\alpha\beta}$ and in the tangential direction as

$$\begin{aligned} -\boldsymbol{f}\cdot\boldsymbol{\tau} = N^{\beta\alpha}_{;\alpha} - S^{\alpha}b^{\beta}_{\alpha} &= a^{\beta\alpha}\left(\frac{\partial W}{\partial\theta^{\alpha}_{|exp}} + \lambda_{,\alpha}\right) \\ &+ 2\nu(d^{\beta\alpha}_{;\alpha} - b^{\beta\alpha}w_{,\alpha}) - 4\nu w a^{\beta\alpha}H_{,\alpha}, \end{aligned} \tag{S9}$$

where $\partial\theta^{\alpha}_{|exp}$ denotes the explicit coordinate dependence of the free energy.

## Free energy and governing equation

The free energy of the membrane is given by

$$\begin{aligned} W = &\underbrace{k_BT[PS]_{sat}\left[\eta\log\eta + (1-\eta)\log(1-\eta)\right]}_{\text{entropic interaction}} - \underbrace{\boldsymbol{f}\cdot\mathbf{z}}_{\text{work done by the forces}} \\ &+ \underbrace{\frac{\gamma[PS]_{sat}}{2}\eta(1-\eta) + \frac{\gamma}{4}|\nabla\eta|^2}_{\text{aggregation}} + \underbrace{\kappa(H - \ell[PS]_{sat}\eta)^2 + \bar{\kappa}K}_{\text{bending}}. \end{aligned} \tag{S10}$$

Here, $\eta$ is the area fraction of PS on the outer leaflet, $[PS]_{sat}$ is the saturation density of PS on the outer leaflet, and we assume that the spontaneous curvature is directly proportional to the density of PS on the outer leaflet. Note that $\boldsymbol{f}$ is the external force density on the membrane, which includes linkers' force and the point force as $\boldsymbol{f} = \boldsymbol{f}_{lin} + f_{pull}\mathbf{z}\delta(\boldsymbol{r} - \boldsymbol{r}_0)$, where $\delta$ is Drac delta function, and $\boldsymbol{r}_0$ is location of applied point force.

The full kinetic equation of $\eta$ on the outer leaflet is given by the following equation

$$\begin{aligned} \eta_t + \underbrace{\nabla\cdot(\boldsymbol{v}\eta)}_{\text{advection}} &= \underbrace{k_{\text{scramblase}}\,e^{\alpha H(s)}\eta^2(1-\eta)}_{\text{scramblase activity}} - \underbrace{k_{P4ATPase}\eta e^{\beta H(s)}}_{\text{P4ATPase activity}} \\ &- \underbrace{\frac{\eta}{F_D}\left[\frac{\gamma}{2[PS]_{sat}}\Delta^2\eta\right]}_{\text{aggregation}} + \underbrace{\frac{\Delta\eta}{F_D}\left[\frac{k_BT}{1-\eta} + 2\kappa\ell^2[PS]_{sat}\eta - \gamma\eta\right]}_{\text{diffusion}} \\ &+ \underbrace{\frac{2\kappa\ell}{F_D}\left[\eta\Delta H - \nabla\eta\cdot\nabla H\right]}_{\text{nonlinear interaction 1}} + \underbrace{\frac{\nabla\eta}{F_D}\cdot\left[\nabla\eta\left(\frac{k_BT}{(1-\eta)^2} + 2\kappa\ell^2[PS]_{sat} - \gamma\right) - \frac{\gamma\nabla(\Delta\eta)}{2[PS]_{sat}}\right]}_{\text{nonlinear interaction 2}}. \end{aligned} \tag{S11}$$

Here, $F_D$ is the hydrodynamic drag on PS, $\eta$ is the area fraction of PS, the first and second terms in RHS denote the kinetics of scramblase and ATPases, the second and third term denotes diffusion and aggregation, and the rest of the terms indicate non-linear interactions between bending, diffusion, and aggregation.

The governing equation for the membrane shape is given by

$$\begin{aligned}
&\underbrace{\kappa\Delta(H-\ell\eta_{\text{sat}}\eta)}_{\text{bending: Laplacian term}}-\underbrace{2H\kappa(H-\ell\eta_{\text{sat}}\eta)^2}_{\text{bending: nonlinear}}+\underbrace{2\kappa(H-\ell\eta_{\text{sat}}\eta)(2H^2-K)}_{\text{bending: curvature coupling}}\\
&-2H\Bigg[\underbrace{k_BT\eta_{\text{sat}}\big\{\eta\log\eta+(1-\eta)\log(1-\eta)\big\}}_{\text{entropic}}\Bigg]+\phi k_{\text{lin}}z\,\mathcal{H}(z-d_0)\\
&+2H\Bigg[\underbrace{\tfrac{\gamma\eta_{\text{sat}}}{2}\eta(1-\eta)+\tfrac{\gamma}{4}|\nabla\eta|^2}_{\text{aggregation: gradient}}\Bigg]-\underbrace{2\nu\big[\boldsymbol{b}:\boldsymbol{d}\big]}_{\text{viscous: strain}}\\
&+\underbrace{2\nu w(4H^2-2K)}_{\text{viscous: curvature}}=\underbrace{p}_{}+\underbrace{2\lambda H}_{\text{capillary}}+\underbrace{\boldsymbol{f}\cdot\boldsymbol{n}}_{\text{Linker's force}}\quad.
\end{aligned}\tag{S12}$$

where, $\mathcal{H}$ is the Heaviside function, and $d_0$ is the cut off length of linkers. The tension evolution in plane is given by

$$\begin{aligned}
&\nabla\lambda+\underbrace{2\nu(\nabla\cdot\boldsymbol{d}-\nabla w\cdot\boldsymbol{b})-4\nu w\nabla H}_{\text{viscous}}+\underbrace{\boldsymbol{f}\cdot\boldsymbol{\tau}}_{\text{Linker's force}}\quad=\\
&-[PS]_{sat}\nabla\eta\Bigg[\underbrace{k_BT\log\frac{\eta}{1-\eta}}_{\text{entropic}}-\underbrace{2\kappa\ell(H-\ell[PS]_{sat}\eta)}_{\text{bending}}\Bigg]\\
&+[PS]_{sat}\nabla\eta\Bigg[\underbrace{\left(\frac{\gamma}{2}(2\eta-1)+\frac{\gamma}{2[PS]_{sat}}\Delta\eta\right)}_{\text{aggregation}}\Bigg].
\end{aligned}\tag{S13}$$

**Governing equations in Linear Monge and numerical implementation**

**Surface representation**

The surface parametrization for a Monge patch is given by

$$\boldsymbol{r}(x,y,t)=x\boldsymbol{i}+y\boldsymbol{j}+z(x,y,t)\boldsymbol{k}.\tag{S14}$$

The tangent and normal vectors are given by

$$\boldsymbol{a}_1=\boldsymbol{i}+z_{,x}\boldsymbol{k},\quad \boldsymbol{a}_2=\boldsymbol{j}+z_{,y}\boldsymbol{k},\quad \boldsymbol{n}=\frac{(-z_{,x}\boldsymbol{i}-z_{,y}\boldsymbol{j}+\boldsymbol{k})}{(1+z_{,x}^2+z_{,y}^2)^{1/2}}.\tag{S15}$$

The surface metric ($a_{\alpha\beta}$) and curvature metric ($b_{\alpha\beta}$) take the following forms

$$a_{\alpha\beta}=\begin{bmatrix}1+z_{,x}^2 & z_{,x}z_{,y}\\ z_{,y}z_{,x} & 1+z_{,y}^2\end{bmatrix},\tag{S16}$$

$$\text{and } b_{\alpha\beta}=\frac{1}{(1+z_{,x}^2+z_{,y}^2)^{1/2}}\begin{bmatrix}z_{,xx} & z_{,xy}\\ z_{,yx} & z_{,yy}\end{bmatrix}.\tag{S17}$$

**Dimensionless governing equations**

Here we summarize the governing equations for the coupled dynamics of the system in the dimensionless form where the dimensionless numbers are presented in table 1. The tangential force balance equation becomes

$$\boldsymbol{\nabla}\tilde{\lambda}-4\tilde{w}\boldsymbol{\nabla}\tilde{H}+2(\boldsymbol{\nabla}\cdot\tilde{\boldsymbol{d}}-\boldsymbol{\nabla}\tilde{w}\cdot\tilde{\boldsymbol{b}})+\tilde{\boldsymbol{f}}\cdot\boldsymbol{\tau}=-\boldsymbol{\nabla}\eta\left[\frac{2\hat{B}\hat{S}}{\hat{T}}\log\frac{\eta}{1-\eta}-\frac{4\hat{L}\hat{S}}{\hat{T}}(\tilde{H}-\hat{L}\hat{S}\eta)-\frac{\hat{A}\hat{B}\hat{S}}{\hat{T}}(2\eta-1)-\frac{\hat{A}\hat{B}}{\hat{T}}\Delta\eta\right],\tag{S18}$$

along with the surface incompressibility relation,

$$\boldsymbol{\nabla}\cdot\tilde{\boldsymbol{v}}=2\tilde{w}\tilde{H}.\tag{1}$$

Table 1: List of dimensionless numbers and their definitions

| Dimensionless Number | Expression | Physical interpretation | Range |
|---|---|---|---|
| $\hat{B}$ | $\frac{k_B T}{\kappa}$ | $\frac{\text{Thermal energy}}{\text{Bending energy}}$ | 0.0125-0.05 |
| $\hat{L}$ | $\frac{\ell}{L}$ | $\frac{\text{Spontaneous curvature length}}{\text{Domain length}}$ | $2 \times 10^{-3}$ |
| $\hat{A}$ | $\frac{\gamma}{k_B T}$ | $\frac{\text{Aggregation coefficient}}{\text{Diffusion coefficient}}$ | 20 |
| $\hat{S}$ | $[PS]_{sat} L^2$ | $\frac{\text{Domain area}}{\text{Protein footprint}}$ | 200 |
| $\hat{T}$ | $\frac{2L^2\lambda_0}{\kappa}$ | $\frac{\text{Membrane tension energy}}{\text{Bending energy}}$ | 0.01-5 |
| $Pe$ | $\frac{\lambda_0 L^2}{\nu D}$ | $\frac{\text{Advection strength}}{\text{Diffusion strength}}$ | 1 |

The normal force balance relation takes the following form

$$\begin{aligned}
&\Delta(\tilde{H} - \hat{L}\hat{S}\eta) + 2(\tilde{H} - \ell L[PS]_{sat}\eta)(2\tilde{H}^2 - \tilde{K}) \\
&- 2\hat{B}\hat{S}\,\tilde{H}\bigg[\{\eta\log\eta + (1-\eta)\log(1-\eta)\} + \frac{\hat{A}}{2}\eta(1-\eta) \\
&+ \frac{\hat{A}}{4\hat{S}}|\boldsymbol{\nabla}\eta|^2\bigg] - 2\tilde{H}\left[(\tilde{H} - \ell[PS]_{sat}L\eta)^2 + \frac{\bar{\kappa}}{\kappa}\tilde{K}\right] \\
&- \hat{T}\big[\tilde{\boldsymbol{b}} : \tilde{\boldsymbol{d}} - w(4\tilde{H}^2 - 2\tilde{K})\big] = \tilde{p} + f_z + \hat{T}\tilde{\lambda}\tilde{H}.
\end{aligned} \tag{S19}$$

The mass conservation of PS is given by

$$\begin{aligned}
&\eta_t + Pe\boldsymbol{\nabla}\cdot(\tilde{\boldsymbol{v}}\eta) = k_{\text{scramblase}}\, e^{\alpha H(s)}\eta^2(1-\eta) \\
&- k_{P4ATPase}\eta e^{\beta H(s)} + \Delta\eta\bigg[\frac{1}{1-\eta} + \frac{2\hat{L}^2\hat{S}}{\hat{B}}\eta - \hat{A}\eta\bigg] \\
&- \eta\bigg[\frac{2\hat{L}}{\hat{B}}\Delta H + \frac{\hat{A}}{2\hat{S}}\Delta^2\eta\bigg] \\
&+ \boldsymbol{\nabla}\eta\cdot\bigg[\boldsymbol{\nabla}\eta\bigg(\frac{1}{(1-\eta)^2} + \frac{2\hat{L}^2\hat{S}}{\hat{B}} - \hat{A}\bigg) - \frac{2\hat{L}}{\hat{B}}\boldsymbol{\nabla}\tilde{H} - \frac{\hat{A}}{2\hat{S}}\boldsymbol{\nabla}(\Delta\eta)\bigg].
\end{aligned} \tag{S20}$$

**Numerical implementation**

We numerically solved the dimensionless governing equations in the linear Monge regime, specifically equations S18 to S20, within a square domain featuring periodic boundary conditions. We performed numerical simulations on a spatially uniform grid of size $64 \times 64$. A finite difference scheme is adopted to solve the transport equation for the protein density (equation S20), whereas the velocity (equation 1 and equation S18) and the shape (equation S19) were solved using a Fourier spectral method [**hasimoto1959periodic**]. We used A semi-implicit scheme for the time marching for the protein density $\eta$ with a time step $\Delta t = 3 \times 10^{-4}$, with the nonlinear terms involving velocity and curvature were treated explicitly. However, the nonlinear aggregation-diffusion terms were treated with linear implicit terms. The resulting transport equation is shown below

$$\begin{aligned}
&\frac{\eta^{n+1} - \eta^n}{\Delta t} + Pe\,\nabla\cdot(\boldsymbol{v}^{\overline{n+1}}\eta^{n+1}) = \\
&\Big[k_{\text{scramblase}}\, e^{\alpha H(s)}\eta^2(1-\eta) - k_{P4ATPase}\eta e^{\beta H(s)}\Big]^{n+1} \\
&+ \nabla^2\eta^{n+1}\bigg[\frac{1}{1-\eta} + \frac{2\hat{L}^2\hat{S}}{\hat{B}}\eta - \hat{A}\eta\bigg]^{\overline{n+1}} - \eta^{n+1}\bigg[\frac{2\hat{L}}{\hat{B}}\nabla^2 H^{\overline{n+1}}\bigg] \\
&\quad + \eta^{\overline{n+1}}\bigg[\frac{\hat{A}}{2\hat{S}}\nabla^4\eta^{n+1}\bigg] \\
&+ \nabla\eta^{n+1}\cdot\bigg[\nabla\eta\bigg(\frac{1}{(1-\eta)^2} + \frac{2\hat{L}^2\hat{S}}{\hat{B}} - \hat{A}\bigg) - \frac{2\hat{L}}{\hat{B}}\nabla H - \frac{\hat{A}}{2\hat{S}}\nabla(\nabla^2\eta)\bigg]^{\overline{n+1}},
\end{aligned} \tag{S21}$$

where the superscript $\overline{n+1}$ indicates the explicit terms for time step $n+1$, for which the currently available values were considered. The explicit terms were further updated using an iterative scheme, and within each iteration, velocity and shape were recalculated for the updated values of protein density. The iterations were performed within a time step until convergence was achieved. For the convergence within a time step, we used a tolerance of $5 \times 10^{-7}$. When the differences between values of variables from successive iterations fell below the tolerance, we considered the values of the variables to be converged in that time step.

**Governing equations in axisymmetry and numerical implementation**

We solved the governing equation (equation S8-S9) in the limit of axisymmetry where $\frac{\partial}{\partial\theta} \approx 0$. The system of equations can be represented in terms of arclength $s$ as shown in Figure 4a. The surface metric and curvature tensor in axisymmetry becomes

$$a_{\alpha\beta} = \begin{bmatrix} 1 & 0 \\ 0 & r^2 \end{bmatrix}, \tag{S22}$$

and

$$b_{\alpha\beta} = \begin{bmatrix} \psi_s & 0 \\ 0 & r\sin\psi \end{bmatrix}. \tag{S23}$$

The mean curvatures and Gaussian curvature simplify as

$$H = \frac{1}{2}\left(\psi_s + \frac{\sin\psi}{r}\right), \quad K = \psi_s\frac{\sin\psi}{r}. \tag{S24}$$

Note that we introduced an angle $\psi$, which is the angle made by the tangent of the membrane with the cortex plane (see Figure 4a). The tangential and normal components of the adhesive force becomes function of $\psi$ as:

$$\boldsymbol{f} = f_s\boldsymbol{e}_s + f_n\boldsymbol{n} \quad \text{where, } f_s = f\sin\psi = -k_{\text{lin}}z\sin\psi$$

$$\text{and } f_n = f\cos\psi = -k_{\text{lin}}z\cos\psi. \tag{S26}$$

Note that, the total adhesive cortex force $\boldsymbol{f} = f_s\boldsymbol{e}_s + f_n\boldsymbol{n}$. Using the free energy given in equation 1, the tangential force balance along the arclength becomes [3, 4, 5]

$$\frac{\partial\lambda}{\partial s} + f_s = \frac{\partial C}{\partial s}\left[2\kappa(H-C)\right]. \tag{S27}$$

Here, $\lambda$ is the Lagrange multiples for area extensibility, and often interpreted as membrane tension [6, 7]. On the other hand, the normal force balance illustrates shape of the membrane, and is given by [3, 4, 5]

$$\begin{aligned} &\frac{1}{r}\frac{\partial}{\partial s}\left(r\frac{\partial(\kappa(H-C))}{\partial s}\right) + 2\kappa(H-C)\left(2H^2-K\right) \\ &\quad - 2H\left[\kappa(H-C)^2\right] = p + f_n + 2\lambda H. \end{aligned} \tag{S28}$$

In equation S28, $p$ is the normal pressure applied to the membrane and $f_n$ is the normal component of the cortex force on the membrane.

We solved the governing equation (equation S27-S28) numerically in an axisymmetric membrane with temporally evolving spontaneous curvature at according to equation S11 and the spatiotemporal density of linkers across the simulation domain. The solution domain and boundary condition is presented in Figure 4. We split the higher-order shape equation into two lower-order equations. We define $M$ such that

$$\frac{M}{r} = \frac{\partial(\kappa(H-C))}{\partial s}, \tag{S29}$$

and use it to express the normal force:

$$\frac{1}{r}\frac{\partial M}{\partial s} + 2\kappa(H-C)\left(2H^2-K\right) - 2H\left[\kappa(H-C)^2\right] = p + f_n + 2\lambda H. \tag{S30}$$

Notably, $L$ can be interpreted as the normal bending stress on the membrane, and we used the boundary condition of $L = 0$ at the center of the membrane, indicating zero point force at the pole. To solve the tangential and normal force balance equation, we used the MATLAB-based boundary value solver (bvp4c). The kinetic equation of spontaneous curvatures and linkers density is solved with explicit time marching. We used a nonuniform grid ranging from 5,000

to 100,000 points across the radial domain, with the finer grid towards the pole. We used a large solution domain size of $10^4$ nm$^2$ compared to MP area to avoid boundary effects.

Ultimately, we solve a system of six ODEs for the membrane shape. Three of these equations arise from the assumption of axisymmetry:

$$r' = \cos\psi \quad z' = \sin\psi \quad r\psi' = 2rH - \sin\psi \tag{S31}$$

Finally, we also solve Equations S27 and S30. We prescribe the following boundary conditions at the pole $s = 0$:

$$r(0^+) = 0,\ M(0^+) = 0,\ \psi(0^+) = 0. \tag{S32}$$

At the edge ($s = S$) we prescribe the boundary conditions:

$$z(S) = 0,\ \psi(S) = 0,\ \lambda(S) = \lambda_0. \tag{S33}$$

**Pulling force on the membrane**

The pulling force on the membrane depends on the density of the linkers protein on the membrane and the vertical displacement from the cortex plane. Note that each linker works as a linear spring and applies a force in the z-direction of $\hat{F} = -k_{\text{lin}}\, z$. With $\phi$ being the area fraction of the linker density, the force per unit area $\boldsymbol{f}_{lin} = \phi\hat{F}\hat{\mathbf{z}}$. The area fraction is obtained by solving the binding and unbinding equation for linker density in time as given by equation 2.

**Spontaneous curvature**

The spontaneous curvature on the other-hand depends on the density of PS on the outer leaflet of the membrane which is governed by equation S11. The area of lipid for PS, $a_{PS}$, is around 0.58 $nm^2$ and and induces a radius of curvature on the membrane about $14.4\ nm$. Therefore the spontaneous curvature of each PS $C_0 \approx 0.07\ nm^{-1}$ [8]. We use the PS kinetics from experiments to propose a spontaneous curvature function as $C(\eta) = \ell[PS] = \ell[PS]_{sat}\eta$, where $\ell = C_0 a_{PS}$. Multiplying the PS kinetics by this constant factor $\ell$ gives us the rate equation for spontaneous curvature. We consider 20% of area fraction, and resulting multiplication factor to convert $C_0$ from $\eta$ becomes 0.014.

**Point force simulation**

We first investigate the response of the linkers when the membrane is deformed with a point force. We used axisymmetric simulation for this case, where point force is applied to the center; the results are presented in Figure 2. The force magnitude is varied from 0.5 pN to 2 pN at the center (Figure 2B,D), and we also varied the value of the time constant ratio (Figure 2A,C). The detachment of the linkers increases with a higher value of $\zeta$, and force magnitude further enhances the unbinding of linkers. The equilibrium concentration of linkers at the center matches well with the theoretical estimation for smaller point forces (Figure 2F). However, this deviates from theoretical estimation for higher force where bending of the membrane dominates.

**Linear Monge Simulation**

We simulate a 2-dimensional membrane influenced by spontaneous curvature induced by PS molecules and pulling forces exerted by linker proteins. The governing equations equation S18-equation S20 are solved over a square membrane patch. Note that the equation for PS transport (equation S20) incorporates the interactions among PS molecules that drive their aggregation on the membrane. Depending on the local concentration of PS, spontaneous curvature is applied, resulting in localized membrane deformation. Numerical methods, detailed in the section of Numerical implementation, are used to solve these equations, providing the spatiotemporal distribution of PS molecules, linker proteins, and the corresponding membrane deformation as hown in Figure 3A,B. Additionally, membrane tension are shown from the simulation results in Figure 3C.

**Axisymmetric simulation**

The majority of the simulations presented in this paper on microparticle formation are in the axisymmetric domain. The assumption here is that the PS is localized in a circular patch and induces membrane deformation as a result of its spontaneous curvature. The resultant deformation is also coupled with the dynamics of linker detachments. The spontaneous curvature is induced by the local concentration of PS that has a curvature-driven feedback, as shown by $\alpha$ and $\beta$ in equation S20. We investigate microparticle formation without curvature-driven feedback, and then investigate the influence of curvature driven feedback on it.

Table 2: Notation used in the model

| Notation | Description | Unit |
|---|---|---|
| $W$ | Free energy density per unit area of the membrane | $\mathrm{pN}\cdot\mathrm{nm}^{-1}$ |
| $\kappa$ | Bending modulus of the membrane | $\mathrm{pN}\cdot\mathrm{nm}$ |
| $s$ | Arclength along the membrane | $\mathrm{nm}$ |
| $\psi$ | Angle made by surface tangent with the horizontal direction | 1 |
| $H$ | Mean curvature | $\mathrm{nm}^{-1}$ |
| $C$ | Spontaneous mean curvature | $\mathrm{nm}^{-1}$ |
| $\boldsymbol{f}$ | Force per unit area between the membrane and the cortex | $\mathrm{pN}\cdot\mathrm{nm}^{-2}$ |
| $f_{pull}$ | Pulling point force | $\mathrm{pN}$ |
| $\hat{F}$ | Force experience by each linker protein | $\mathrm{pN}$ |
| $k_{lin}$ | linear spring constant of the linker | $\mathrm{pN}\cdot\mathrm{nm}^{-1}$ |
| $p$ | Normal pressure acting on the membrane | $\mathrm{pN}\cdot\mathrm{nm}^{-2}$ |
| $\lambda$ | Membrane tension | $\mathrm{pN}\cdot\mathrm{nm}^{-1}$ |
| $k_{scramblase}$ | scramblase rate constant of PS | $\mathrm{s}^{-1}$ |
| $k_{P4ATPase}$ | flipping rate constant of PS | $\mathrm{s}^{-1}$ |
| $[PS]_{sat}$ | equilibrium concentration of of PS | $\mu\mathrm{M}$ |
| $k_{on}$ | Association rate constant of linkers | $\mathrm{s}^{-1}$ |
| $k_{off}$ | Dissociation rate constant of linkers | $\mathrm{s}^{-1}$ |
| $\gamma$ | Effective interaction energy of PS | $\mathrm{pN}\cdot\mathrm{nm}$ |
| $\nu$ | membrane viscosity | $\mathrm{pN}\cdot\mathrm{s}\cdot\mathrm{nm}^{-1}$ |
| $F_D$ | hydrodynamic drag force resisting mobility of PS | $\mathrm{pN}\cdot\mathrm{nm}^{-2}$ |

**Without curvature driven feedback**

In this set of simulations $\alpha$ and $\beta$ is considered zero, therefore local curvature has no direct impact on spontaneous curvature. The results in Figure 5–Figure 7 do not include curvature driven feedback. Therefore, spontaneous curvature depends solely on the PS concentration, and membrane curvature have one-way coupling with spontaneous curvature. We see the formation of microparticles depends on various parameters like PS kinetics (Figure 5), Linkers' stiffness (Figure 6), bending rigidity and membrane tension (Figure 7). In all these simulations, we observed a timescale imposed by the linkers' depletion kinetics, and dynamics of membrane shape is governed by the timescale, and we saw a similar trend in the temporal dynamics of the membrane tension as well as shown in Figure S2 and Figure S3, where the role of PS kinetics and linkers' stiffness $k_{lin}$ were highlighted.

**With curvature driven feedback**

We investigated how the strength of curvature driven feedback on PS kinetics could influence successful MP formation. To do this, we took conditions that were already favorable for successful MP formation from Figure 5,6, which are WT PS kinetics and $\zeta = 1$ and now tested how the strength of curvature dependent feedback ($\alpha$ and $\beta$) and linker stiffness play a role in successful MP formation (Figure S1). In these simulations, $\alpha$ was chosen greater than $\beta$ to ensure that scramblase activity was dominant and that PS-induced spontaneous curvature would be similar to the WT kinetics. We observed that the maximum deformation at the center of the membrane depended on the value of linker stiffness and changes to the value of curvature driven feedback had a small effect Figure S1C. The fraction of bound linkers depended on the value of linker stiffness (Figure S1D). The effective change in spontaneous curvature was not large in the presence of curvature driven feedback (Figure S1A) and in all cases tested, we observed successful MP formation (Figure S1B).

## Supplementary Tables

The notation Figure 2 and values of parameters are summarized below in table 3.

Table 3: List of parameters

| Notation | Description | Range |
|---|---|---|
| $\kappa$ | Bending modulus of the membrane | $40 - 600$ pN $\cdot$ nm $(10 - 150$ k$_B$T) [9] |
| $\lambda_0$ | Membrane tension at the boundary | $0.001 - 0.1$ pN $\cdot$ nm$^{-1}$ [10, 7] |
| $a_{\text{coat}}$ | Coat area of the PS domain based on MP sizes | $2.5 \times 10^4 - 5 \times 10^4$ nm$^2$ [11] |
| $k_{\text{lin}}$ | Linear spring constant of cortex | $0.01 - 0.1$ pN $\cdot$ nm$^2$ [12] |
| $k_{on}$ | Association rate constant of the linkers | $0.01 - 0.1$ s$^{-1}$ [12, 13, 14] |
| $k_{off}$ | Dissociation rate constant of the linkers | $0.01 - 0.1$ s$^{-1}$ [12, 13, 14] |
| $k_{scramblase}$ | Rate constant PS flipping through scramblase | $0.910 - 2.25$ s$^{-1}$ [15] |
| $k_{P4ATPase}$ | rate constant for P4ATPase activity | $0.08 - 0.2045$ s$^{-1}$ [15] |
| $\nu$ | membrane viscosity | $5 \times 10^{-6}$ pN $\cdot$ s $\cdot$ nm$^{-1}$ |
| $\ell$ | spontaneous curvature of single PS | 0.014 nm$^{-1}$ [16] |
| $a_{PS}$ | area occupied by single PS | 0.58 nm$^2$ |

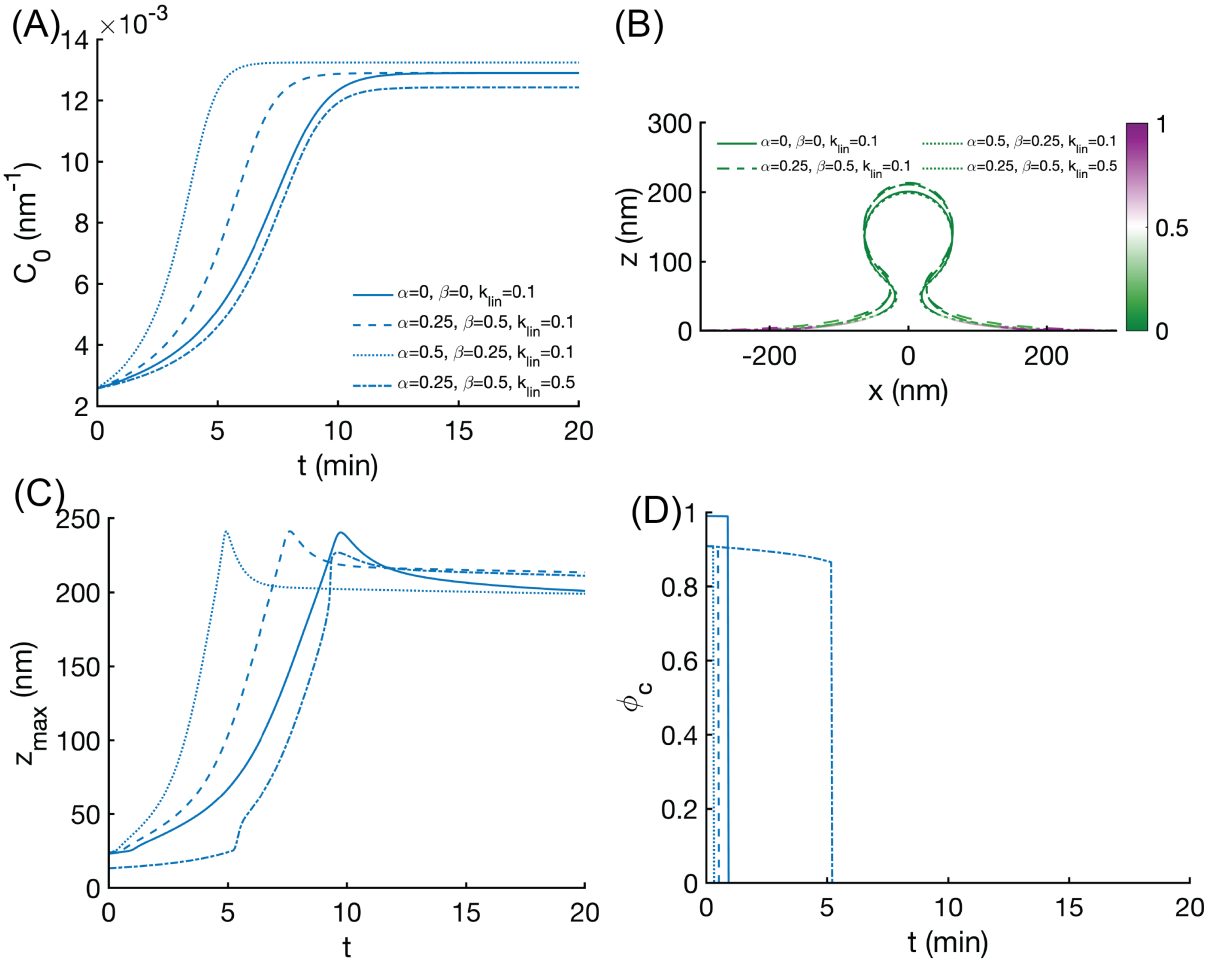


Figure S1: **Effect of curvature-driven feedback.** We used non-zero values of $\alpha$ and $\beta$ in equation S11. We tested two different values of $\alpha$, and $\beta = 1$ because the exact values of these parameters are not known. (A) The curvature-driven feedback serves to very slightly alter the kinetics of PS-induced spontaneous curvature at the center of the membrane as denoted by $C_0$. (B) Membrane shapes at a final time for different values of $\alpha$, $\beta$, and $k_{lin}$ are shown. (C) Change of maximum displacement of the membrane as a function of time (in min) for four different combinations $\alpha$ and $\beta$. (D) Change in $\phi$ at the center of the membrane as a function of time (min) for the combinations of $\alpha$ and $\beta$ shown in (A). In all these simulations, the bending modulus was $\kappa = 20k_BT$, tension was $\lambda = 0.001$ pN/nm, linkers' stiffness $k_{lin} = 0.1$ pN/nm and spontaneous curvature area was 50265 nm$^2$.

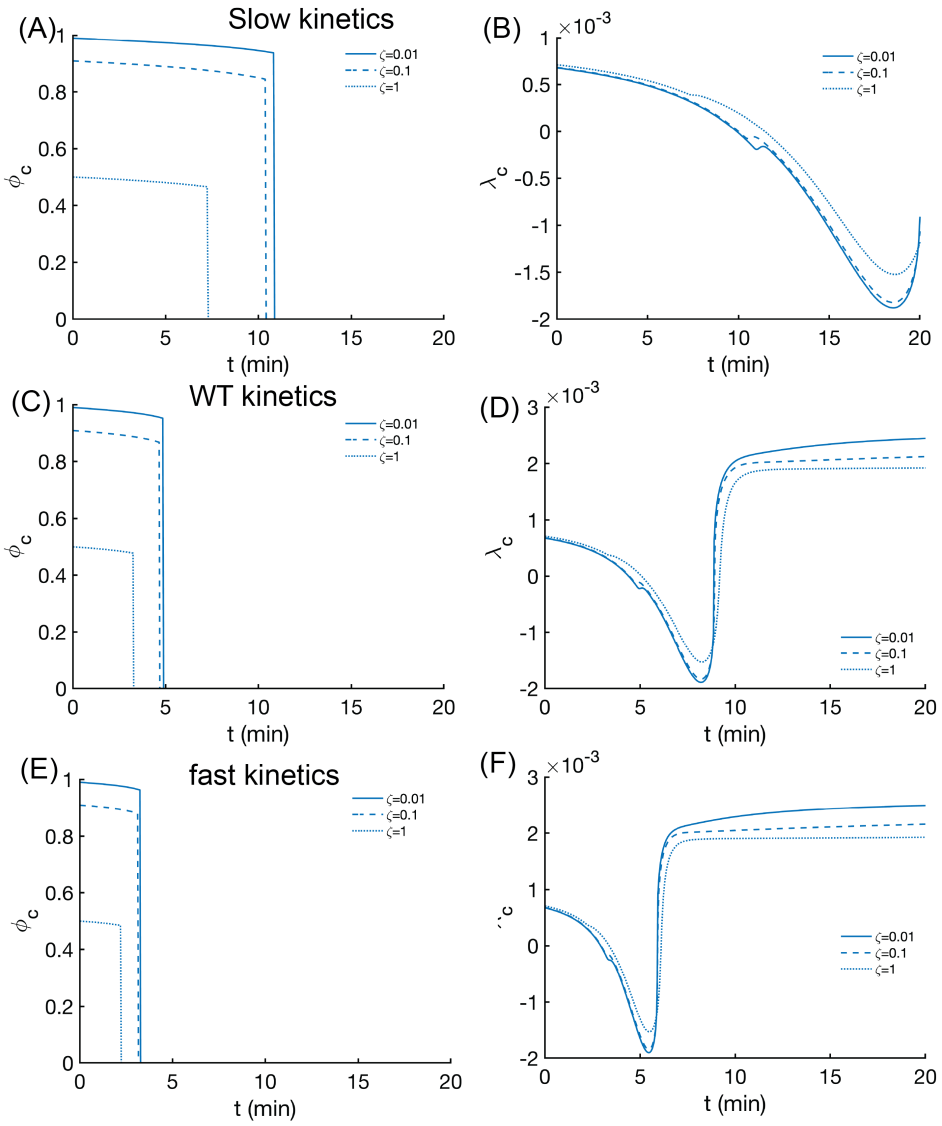


Figure S2: **Role of PS kinetics on the membrane tension.** The role of PS kinetics is presented here for all three values of $\zeta$. Linkers' protein density at the center of the membrane (A,C,E)is plotted with time, and corresponding membrane tension at the center of the membrane is shown (B,D,F). The time scale of linkers' depletion at the center of the membrane, as the PS kinetics changes from slow (A) to WT (B) and fast (C), corresponding tension at the center of the membrane, are shown in (B),(D), and (F). In all these simulations, the bending modulus $\kappa = 20k_BT$ and tension at the boundary $\lambda$ = 0:001 pN/nm, and linkers' stiffness $k_{lin} = 0.1$ pN/nm.

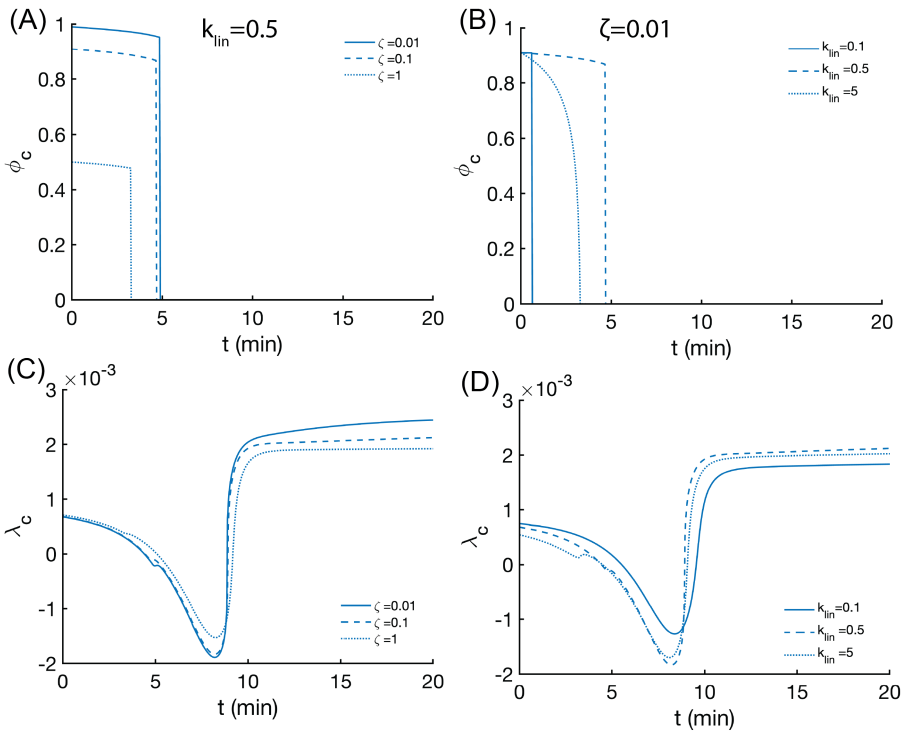


Figure S3: **Role of linker stiffness and time constant ratio on the membrane tension.** The timescale of depletion of linkers at the center of the membrane is shown for different values of time constant ratio (A) and linkers stiffness (B). Tension at the center of the membrane for different values of $\zeta$ (C) and for different values of kinkers' stiffness. In all these simulations, the bending modulus $\kappa = 20k_BT$ and tension $\lambda_0$ = 0.001 pN/nm.

## References


[1] Steigmann D. J. "Fluid films with curvature elasticity". *Arch. Ration. Mech. Anal.* 150 (2 1999-12-01), pp. 127–152.

[2] Kreyszig E. *Introduction to differential geometry and Riemannian geometry*. Mathematical Expositions. Toronto, ON, Canada: University of Toronto Press, 1969-04. 382 pp.

[3] Steigmann D. "Fluid films with curvature elasticity". *Arch. Ration. Mech. Anal.* 150 (2 1999-12-01), pp. 127–152.

[4] Hassinger J. E. et al. "Design principles for robust vesiculation in clathrin-mediated endocytosis". *Proceedings of the national academy of sciences* 114 (7 2017-02-14), E1118–E1127.

[5] Mahapatra A., Saintillan D., and Rangamani P. "Transport phenomena in fluid films with curvature elasticity". *J. Fluid Mech.* 905 (A8 2020-12-25).

[6] Rangamani P., Mandadap K. K., and Oster G. "Protein-induced membrane curvature alters local membrane tension". *Biophys. J.* 107 (3 2014-08-05), pp. 751–762.

[7] Rangamani P. "The many faces of membrane tension: Challenges across systems and scales". *Biochim. Biophys. Acta Biomembr.* 1864 (7 2022-07-01), p. 183897.

[8] Fuller N., Benatti C. R., and Rand R. P. "Curvature and bending constants for phosphatidylserine-containing membranes". *Biophys. J.* 85 (3 2003-09), pp. 1667–1674.

[9] Monzel C. and Sengupta K. "Measuring shape fluctuations in biological membranes". *J. Phys. D Appl. Phys.* 49 (24) 2016-05-12), p. 243002.

[10] Lipowsky R. "Spontaneous tubulation of membranes and vesicles reveals membrane tension generated by spontaneous curvature". *Faraday Discuss.* 161 (0 2013-01-24), pp. 305–331.

[11] Piccin A., Murphy W. G., and Smith O. P. "Circulating microparticles: pathophysiology and clinical implications". *Blood Rev.* 21 (3 2007-05), pp. 157–171.

[12] Alert R. et al. "Model for probing membrane-cortex adhesion by micropipette aspiration and fluctuation spectroscopy". *Biophys. J.* 108 (8 2015-04-21), pp. 1878–1886.

[13] Tsai F.-C. et al. "Ezrin enrichment on curved membranes requires a specific conformation or interaction with a curvature-sensitive partner". *Elife* 7 (2018-09-20), e37262.

[14] Fritzsche M., Thorogate R., and Charras G. "Quantitative analysis of ezrin turnover dynamics in the actin cortex". *Biophys. J.* 106 (2 2014-01-21), pp. 343–353.

[15] Watanabe R. et al. "Single-molecule analysis of phospholipid scrambling by TMEM16F". *Proc. Natl. Acad. Sci. U. S. A.* 115 (12 2018-03-20), pp. 3066–3071.

[16] Hirama T. et al. "Membrane curvature induced by proximity of anionic phospholipids can initiate endocytosis". *Nat. Commun.* 8 (1 2017-12-09), pp. 1–14.